IEEE Access
Multidisciplinary | Rapid Review | Open Access Journal

Received February 20, 2020, accepted March 15, 2020, date of publication March 19, 2020, date of current version March 31, 2020.

*Digital Object Identifier 10.1109/ACCESS.2020.2981953*

# Spatiotemporal Characterization of Users' Experience in Massive Cognitive Radio Networks

**SAMUEL D. OKEGBILE[1], (Student Member, IEEE), BODHASWAR T. MAHARAJ[1], (Senior Member, IEEE), AND ATTAHIRU S. ALFA[1,2], (Member, IEEE)**

[1]Department of Electrical, Electronic, and Computer Engineering, University of Pretoria, Pretoria 0002, South Africa
[2]Department of Electrical and Computer Engineering, University of Manitoba, Winnipeg, MB R3T 2N2, Canada

Corresponding author: Samuel D. Okegbile (samokegbile@gmail.com)

This work was supported by the SENTECH Chair in Broadband Wireless Multimedia Communications (BWMC), Department of Electrical, Electronics, and Computer Engineering, University of Pretoria, South Africa.

**ABSTRACT** The need to capture the actual network traffic condition and fundamental queueing dynamics in a massive cognitive radio network (CRN) is important for proper analysis of the intrinsic effects of spatial distribution while capturing the essential temporal distribution properties of the network. In massive CRN, many users, including primary and secondary users, transmit on scarce spectrum resources. While primary users (PUs) are delay-sensitive users that require prioritized access over secondary users (SUs), carrying out analysis that captures this property becomes imperative if users' service experience is to be satisfactory. This paper presents priority conscious spatiotemporal analysis capable of characterizing users' experience in massive CRN. Users in the primary priority queue were considered to have pre-emptive priory over users in the virtual and secondary priority queues. A Geo/G/1 discrete-time Markov chain queueing system was adopted to characterize both primary and secondary priority queues, while the virtual priority queue was analyzed as part of the secondary priority queue. Using the tools of stochastic geometry and queueing theory, the user's coverage probability was determined while the delay experienced by each class of users in the network was obtained using existing results. Through the obtained delay for each class of users in the network, the corresponding quality of service was also obtained. The results obtained show that the proposed framework is capable of accurately characterizing users' service experience in massive CRN.

**INDEX TERMS** Delay, service experience, spatiotemporal analysis, quality of service, transmission success.

## I. INTRODUCTION

With the rapid evolution of wireless communications and technologies, the number of devices and applications accessing scarce spectral resources continues to increase. Many devices are expected to be connected and to communicate via wireless networks as the next era of development in e-health, machine-to-machine communications and internet of things (IoTs) approaches. In view of this expected increase in the number of devices requiring access to the network, all devices will not be able to access the spectral resources at the same time without causing disruptive interference on the network, leading to spectrum usage degradation. As a result of this, interference management and control in wireless networks have been receiving a lot of attention in the last decades. For instance, in the cognitive radio network (CRN), unlicensed users are allowed to make use of channels belonging to licensed users opportunistically, provided that their transmissions will not cause excessive disruption to the activities of licensed users. Similar requirements have now been applied in other wireless network paradigms, such as heterogeneous and cellular networks.

In order to prevent interference to the activities of the licensed users, while still ensuring efficient usage of the scarce spectrum resources, various methods have been adopted in CRN. Preliminary works have adopted the use of the discrete-time ALOHA protocol where the presence of more than two transmitting nodes at any given slot results in a collision. This approach fails to capture the information-centric interactions among network nodes accurately [1].

The associate editor coordinating the review of this manuscript and approving it for publication was Emrecan Demirors.

Recently, the adoption of stochastic geometry (SG) has been demonstrated to be useful in providing accurate and tractable analysis capable of modeling interference in the networks. With the adoption of SG in CRN, primary users' (PUs) protection regions are introduced within which no secondary user (SU) is allowed to transmit. SUs can then transmit on the locations outside the tagged PU protection region if not occupied by other PUs or wait until a PU becomes inactive. However, most of the analyses obtained through the use of SG were achieved under full buffer assumption, an assumption that did not capture the actual network traffic condition. In reality, users are not always transmitting, while some users of the spectrum also require higher priority, depending on the data and channel access requirements.

This actual network traffic condition as well as the information-centric interactions can be captured well by modeling the dynamics from both the temporal and spatial domains; hence, recent efforts have been looking into combining stochastic geometry and queueing theory. With the introduction of PUs' protection zones, SUs' access to channels now depends on active PUs transmission duration - a parameter that also depends on both intra-network and inter-network interference. These intra-network and inter-network interference among different users, however, can lead to interacting queues. Thus, investigating the relationship between PUs and SUs is imperative if one is to understand users' quality of service (QoS) in a massive CRN.

The presence of interacting queues means the queueing status at both primary and secondary priority queues as well as users' active states vary from one user to another even if the packet arrival rate is assumed to be the same for all users. Hence, analysis of networks with interacting queues is known to be very difficult [2]. Interference characterization in such a system is not straightforward, since the received signal-to-interference plus noise ratio (SINR) depends on various stochastic processes such as users' distributions, users' arrivals and queueing dynamics, which can only be characterized through distribution.

In this paper, PUs are users that require immediate access to channels and therefore enjoy non-negotiable priority to access channels at any point in time, while SUs are users with less priority whose access to the channel can be delayed, albeit with the necessary efforts being made to satisfy their QoS requirements. We also define a massive CRN as a network in which multiple users gain access to transmit on each band of the spectral resources based on their arrival times and priority classes. In the next subsection, we review some of the related works.

### A. RELATED WORK

Interference characterization in CRN was carried out in [3]–[8] using SG. In [3], [4], threshold-based opportunistic spectrum access was adopted to characterize spatial throughput and opportunity, while interference was characterized in two-tier cognitive networks by using the exclusion region in [5]. Similarly, interference and throughout modeling was carried out in multichannel CRN in [6], [7]. With the tool of SG, these works derived tractable analysis for various performance metrics of interest under full buffer assumption. This assumption implies that all transmitters are considered always to have at least a packet to transmit, an assumption that failed to capture the actual network traffic condition and fundamental queueing dynamics at each transmitter.

In order to capture the network random traffic, the relationship between the spatial location of base stations (BSs)/access points (APs) and their temporal traffic dynamic was captured in small cell networks [1], [9], [10], heterogeneous cellular networks [11], IoT enabled cellular networks [12], [13], Poisson network [2], [14] and multi-cell mobile edge computing enabled stochastic wireless networks [15]. While the introduction of randomness in the temporal domain further complicates network analysis, relaxing the full buffer assumption is crucial to next generation wireless systems [1].

With the adoption of both queueing theory and SG, the arrival of packets at each BS/user was regarded as an independent Bernoulli process in [1], [2], [9]–[11], [14] and independent Poisson arrival processes in [13], [16] while the BS/AP deployment and users' locations were modeled as an independent Poisson point process (PPP) [1], [9], [11]–[13]. Each BS was also assumed to have an infinite buffer capacity to store incoming packets in [1], [10]. In [11], the queueing system at any typical transmitter was modeled as Geo/G/1, while [12] applied a two-dimensional Geo/PH/1 discrete-time Markov chain (DTMC) at each device in an uplink scenario owing to its simplified memory-less inter-arrival process, as well as its general departure process that took into consideration the interference-based interactions between the IoT queues. Pre-emptive resume M/G/1/K was similarly applied in [19] because of the need to minimize cognitive users' handoff delay and service time. The network random traffic was modeled using a discrete time queueing system where time is segmented into slots with packet arrival and departure assumed to take place in each time slot. Similarly, queue performance of CRN was studied in [20], while SU throughput in the presence of PU QoS requirement was maximized in [21].

The integration of queueing theory and stochastic geometry in achieving the spatiotemporal analysis of network parameters means, the expressions for various performance metrics of interest can be obtained. Delay distribution analysis has been obtained for random scheduling [10], [11], round-robin scheduling [10], [11], as well as first-in-first-out scheduling [10]. Packet throughput analysis was also obtained in [9]. It is worth noting that the analyses in [1], [2], [9]–[16] were based on first-come-first-serve (FCFS), round-robin or random selection discipline in which transmitting nodes are differentiated based on either their temporal arrival or simply random selection principle rather than their priority classes. Hence, priority-based spatiotemporal analysis especially in CRN remains an open issue. Priority jump strategy was adapted in the D2D cellular network in [17], while [18] considered priority among heterogeneous SU packets in CRN. However, characterizing users' experience

in a typical CRN with priority queues while still capturing the network spatio-temporal features has not been considered before.

The efforts closest to our work are those of [18]–[22]. In [18], [19]; pre-emptive M/M/1 and pre-emptive resume priority M/G/1/K queueing systems were respectively proposed to model CRN and analysis was subsequently obtained for the total average service time of cognitive users in the network. However, the analysis presented did not include the intrinsic effects of spatial distribution and failed to capture the essential temporal distribution properties of the network. The authors in [22] proposed a priority-aware spatiotemporal framework for massive IoT networks' characterization under an uplink network scenario where packets generated at each IoT device were differentiated based on their priority classes. A two-dimensional Geo/PH/1 DTMC was applied at each device to track the priority class being served at any given time slot.

### B. CONTRIBUTIONS

In this paper, we consider a massive CRN in which PUs have pre-emptive priorities to access channels at the start of any time slot and can interrupt the service of any currently active SUs. The interrupted SUs are immediately moved to a virtual queue and enjoy higher priority over newly arrived SUs in order to resume their unfinished services or transmissions. The contributions of this paper are hence summarised as follows:

- We obtained tractable analysis for the service rate - expressed as the conditional coverage probability at any primary and secondary receivers while considering interference from other transmitters with non-empty buffers as in a massive CRN. Coverage probability analysis was carried out for two cases: i.) baseline CRN - where both PUs and SUs transmit with different power, and ii.) simplified CRN - where PUs and SUs transmit with the same transmit power. The coverage probabilities obtained provide insights into the probability of successful transmission in each network.
- We applied vacation and pre-emptive priority-based queueing system approaches and the tool of SG to characterize the relationship between primary and secondary priority classes. Owing to its simplified inter-arrival time in discrete time queueing system and its ability to overcome lack of memory property assumption for service time [23], we adopted the use of a Geo/G/1 DTMC queueing system to model both primary and secondary priority queues. The server is the channel that can be dynamically accessed by SUs opportunistically, provided that the channels' constraints are satisfied and that the primary queue is empty.
- We obtained tractable closed-form expressions for the mean delay in both networks, taking into consideration the mean time each transmitter spends in the system, including the time spent in the queue waiting for a service opportunity.

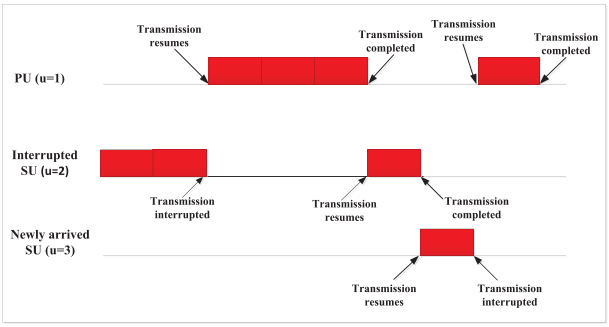


**FIGURE 1.** Channel access in pre-emptive priority queueing system.

- Based on the delay experienced by a typical user in each priority queue, we investigated users' QoS in both primary and secondary queues and presented the results of the analysis.

Some of the common notations used in this paper are presented in Table 1. The remainder of this paper is organized as follows: Section II describes the network model, including the description of the proposed spatiotemporal model. In Section III, we present the analysis of such a spatiotemporal model, while the performance analysis was carried out in Section IV. Section V presents the numerical simulations and results, while Section VI concludes the paper.

## II. NETWORK MODEL

We considered a typical massive CRN with two classes of transmitters - primary transmitters (PTs) and secondary transmitters (STs). All PT and ST arrival rates follow an independent Bernoulli process with parameter $\xi_u$, $\forall u = [p, s]$, where $u = p$ refers to PT arrival with higher priority and $u = s$ refers to ST arrival with lower priority. The inter-arrival times between PTs is said to follow the geometric process with parameter $\xi_p = [0, 1]$ packet per time slot. Similarly, the inter-arrival times between STs is said to follow an independent geometric process with parameter $\xi_s = [0, 1]$ packet per time slot. In any typical location of the Euclidean space (i.e. $L \in R^2$), no ST is allowed to transmit in the presence of any PT. In the absence of PTs, access is granted to secondary queue and STs transmission follow the FCFS approach. Such transmission is immediately interrupted and the secondary queue is expected to proceed on vacation if any PT arrives at the primary queue before the completion of such an ST's service. In other words, when the channel is not available for a class of users, such a class of users will see the channel as being on vacation. As shown in Fig. 1, an interrupted ST is moved to the virtual queue and is granted pre-emptive resume priority over the newly arrived STs immediately the primary queue is empty.

PTs and STs are assumed to be distributed following two independent PPPs $\Phi_p$ and $\Phi_s$ with intensities $\lambda_p$ and $\lambda_s$ respectively, while each primary receiver (PR) and secondary receiver (SR) respectively are uniformly located within region $L$ of radius $D$, where $D$ is defined as the

**TABLE 1. Common notations used.**

| Notation | Definition |
|---|---|
| $\Phi_p$ | Point process representing baseline PUs |
| $\Phi_s$ | Point process representing baseline SUs |
| $\lambda_p^1$ | The intensity of active PUs transmitting in the same slot |
| $\lambda_s^1$ | The intensity of active SUs transmitting in the same slot |
| $\alpha$ | Path loss exponent |
| $P_p, P_s$ | Primary and secondary users' transmit powers |
| $\varrho$ | Thermal noise power known to be independent of other elements |

radius of coverage region implemented around each active transmitter. Each PR associates with the closest PT, while each SR also associates with its nearest ST following the single connectivity method. Any typical transmitter transmits only when it has a packet to send and remains inactive when there is no packet to send. In order to avoid any unnecessarily complicated analysis, we assumed a discrete time queueing system in which time is segmented into equal time slots $t = 1 \ldots \infty$. PT and ST arrivals and departures can, therefore, be said to occur within the time slot boundaries. That is, any transmitter's departure can only occur in the interval $(t^-, t)$ and arrival, including transmission resume, can only occur in the interval $(t, t^+)$. We further assumed that any active transmitter has a random number $n$ of packets to transmit and that each of these packets requires one slot to be transmitted. The number of packets of any transmitter is hence a positive random variable given as

$$a(n) = P[\text{the number of packets of a transmitter} = n], \quad n \geq 1, \tag{1}$$

and its generating function can be expressed as

$$A(z) = \sum_{n=1}^{\infty} a(n) z^n. \tag{2}$$

For $U$ number of priority classes in the network, each with its respective queue, the *uth* priority queue's vacation and service periods can be characterized using general distribution where a typical transmitter is either in active mode when currently holding access to the channel or on vacation mode when the channel is currently being used by another transmitter in a higher priority queue (i.e., the channel is unavailable for the *uth* priority class). Hence, when a typical active transmitter in the priority queue $Q_u$ is currently accessing the channel, other priority queues $Q_m$, $m = u + 1, \ldots U$ are on vacation (i.e. do not have access to channel).

Such a channel access and utilization mechanism can be expressed as an absorbing Markov chain in which the channel can be said to be looping in transient states when serving higher priority transmitters. When all higher priority transmitters have been served and their corresponding queues are empty, the channel can be said to have returned from vacation, hence, in the absorbing state. In the case of three priority queues - primary queue $Q_1$, virtual queue $Q_2$ and secondary queue $Q_3$, the channel transient and absorbing states depend on the *uth* priority queue. A typical *uth* priority queue is not aware of the lower priority queue, i.e. $Q_n$ is not aware of $Q_m$, $m \geq n + 1$. Hence, for a virtual priority queue, the channel is said to be looping in transient states when serving the primary queue and in absorption state when the primary queue is empty, thus, serving the virtual queue. This means that, at $Q_1$, absorption represents the case where the primary queue is empty and channel access is given to the $Q_m$ priority queue, while at $Q_m$, absorption means the channel is available for transmission. Similarly, for a secondary priority queue, the channel is said to be looping in transient states when serving either $Q_1$ or $Q_2$, but in absorption state when both $Q_1$ and $Q_2$ are empty, thus, serving the secondary queue.

The queueing dynamics in the primary priority queue is straightforward and is only dependent on the arrival rate and service time in $Q_1$. The queueing dynamics in the secondary queue is, however, dependent on primary arrival and service rates as well as the arrival rate and service time in $Q_3$. This service time is modeled as a positive random variable and is affected by users' coverage probabilities in the network. If a transmission is unsuccessful in any time slot, such transmission is repeated in the next time slot subject to priority access constraints. The queue dynamics of any primary priority queue is given as

$$H_p(t+1) = [H_p(t) + \xi_p(t) - D_p(t)]^+, \tag{3}$$

where $(H + \xi - D)^+ \triangleq \max\{0, H + \xi - D\}$. The queue dynamics of any secondary priority queue is given as

$$H_s(t+1) = \begin{cases} [H_s(t) + \xi_s(t) - D_s(t)]^+ & \text{if } H_p(t) = 0 \\ [H_s(t) + \xi_s(t)]^+ & \text{if } H_p(t) > 0, \end{cases} \tag{4}$$

where $H_u(t)$ is the number of *uth* priority class transmitter in the system (including those currently transmitting), $\xi_u(t)$ and $D_u(t)$ represents the arrivals and departure in the *uth* priority queue at any time slot $t$. The channel is said to have returned from vacation (i.e. available for secondary transmission, if at least one ST is waiting) in time slot $t$ if the primary queue is empty at the beginning of time slot $t$.

### A. SIGNAL-TO-NOISE PLUS INTERFERENCE RATIO ANALYSIS IN THE PRIMARY NETWORK

In each time slot, each PT with non-empty buffer sends its head-of-line packet with active indicator $\rho_p$. Each PT is assumed to be aware of the transmission success of the sent packet at its pair PR. For every failed transmission attempt in each time slot say $t$, the packet is returned to the head of the queue and retransmitted during the next time slot $t + 1$. A successful packet is removed from the PT's buffer. PTs with

empty buffers are removed from the queue until the primary queue is empty; this, provides transmission opportunities for SUs while reducing accumulated interference in the network.

*Definition 1:* The association region of any typical PT $x_k^p \in \Phi_p$ is given as

$$\varsigma(x_k^p) = \{y \in R^2 : |y - x_k^p| \leq |y - x_i^p|, \forall i \in \{1 \dots n\}\}. \quad (5)$$

*Remarks:* Under Rayleigh fading assumption $h \sim \exp(1)$ and given that all transmitters belonging to the same priority class transmit with the same transmit power, the closest PT $x_k^p$ to any tagged PR $y$ generates the highest power at the tagged PR. This condition is the same for ST and SR.

The SINR received at any tagged PR location $y_k^p$ during any slot $t$ is affected by interference from neighbouring PTs (except the tagged PT, $x_k^p$) and all active STs. Its derivation is given as (6), as shown at the bottom of this page. $\|x_k^p\| = |y - x_k^p|$ and $\rho_{p,t}$ is an indicator representing the active/inactive state of a typical PT $x_i^p \in \Phi_p$ in time slot $t$. Similarly, $\rho_{s,t}$ is an indicator representing the active/inactive state of a typical ST $x_i^s \in \Phi_s$. It is worth noting that the indicators $\rho_{p,t}$ and $\rho_{s,t}$ are both spatial and temporal dependent.

### B. SIGNAL-TO-NOISE PLUS INTERFERENCE RATIO ANALYSIS IN THE SECONDARY NETWORK

Each ST with a non-empty buffer but with access to transmission in slot $t$ sends its head-of-line packet with active indicator $\rho_s$ under the assumption that the tagged ST is aware of the transmission success of the sent packet at its paired SR. For every failed transmission attempt in each time slot say $t$, the packet is returned to the head of the user's queue and retransmitted during the next time slot $t + 1$, provided that the class priority constraints are satisfied. A successful packet is removed from the ST's internal buffer and STs with empty buffers are removed from the secondary queue. The SINR received at any typical SR $y_k^s$ located at the origin at any time slot $t$ is also affected by interference from all active PTs and the neighbouring STs and can be given as (7), as shown at the bottom of this page.

The success probability of a typical transmitter is given as $P(\gamma_t) = pP(\nu_t \geq \theta | \Phi = \Phi_p \cup \Phi_s)$, where $p$ is the probability that the tagged transmitter transmits at time slot $t$.

## III. ANALYSIS

In this section, we present the analysis for conditional coverage probability at any primary or secondary receiver. We then provide our analysis for the adopted queueing system, taking into consideration the pre-emptive priority of the primary queue and channel vacation policy.

### A. CONDITIONAL COVERAGE PROBABILITY ANALYSIS

The coverage probability at any typical receiver is the probability that the received signal ($\nu$) is not less than the predefined threshold $\theta$. The conditional coverage probability at any typical PR located at the origin is thus given as

$$\mu_{y_k^p,t} = P(\nu_{y_k^p,t} \geq \theta_p | \Phi, \forall \Phi = \Phi_p \cup \Phi_s). \quad (8)$$

*Lemma 1:* Given that a tagged PR $y_k^p \in \Phi_p$ is located at the origin of a disk and conditioned on the spatial realization $\Phi = \Phi_p \cup \Phi_s$, the coverage probability in time slot $t$ is expressed as

$$\mu_{y_k^p,t} = e^{-\frac{\theta_p \|x_k^p\|^\alpha}{\varphi}} \prod_{x_i^p \in \Phi_p \setminus x_k^p} \left(1 - \frac{E[\rho_{p,t}|\Phi]}{1 + \|x_i^p\|^\alpha / \theta_p \|x_k^p\|^\alpha}\right) \times \prod_{x_i^s \in \Phi_s} \left(1 - \frac{\vartheta E[\rho_{s,t}|\Phi]}{1 + \|x_i^s\|^\alpha / \theta_p \|x_k^p\|^\alpha}\right), \quad (9)$$

where $\varphi = \dfrac{P_p}{\varrho}$ and $\vartheta = \dfrac{P_s}{P_p}$. If all classes of transmitters transmit with the same transmit power as in the simplified CRN scheme, the conditional coverage probability as $\varrho \to 0$ is expressed as

$$\mu_{y_k^p,t} = \prod_{x_i^p \in \Phi_p \setminus x_k^p} \left(1 - \frac{E[\rho_{p,t}|\Phi]}{1 + \|x_i^p\|^\alpha / \theta_p \|x_k^p\|^\alpha}\right) \times \prod_{x_i^s \in \Phi_s} \left(1 - \frac{E[\rho_{s,t}|\Phi]}{1 + \|x_i^s\|^\alpha / \theta_p \|x_k^p\|^\alpha}\right). \quad (10)$$

*Proof:* The proof is similar to the analysis provided in [1] and is presented in Appendix A for completeness.

Now, we derive a closed-form expression for $\mu_{y_k,t}$.

*Assumption 1:* We assumed independent coverage probability in each time slot.

*Remarks* - According to [11], [12], SINR involves a negligible temporal correlation across time slots and can be assumed to be independent at each slot. Hence, we drop the notation $t$. Following Assumption 1, we present the closed-form expression for the primary coverage probability.

*Lemma 2:* The coverage probability of a tagged PT $x_k^p \in \Phi_p$ in a primary queue located within region $L \in R^2$ is given as

$$\nu_{y_k^p,t} = \frac{P_p h_{x_k} \|x_k^p\|^{-\alpha}}{\varrho + \sum_{x_i^p \in \Phi_p \setminus x_k^p} P_p \rho_{p,t} h_{x_i} \|x_i^p\|^{-\alpha} + \sum_{x_i^s \in \Phi_s} P_s \rho_{s,t} h_{y_i} \|x_i^s\|^{-\alpha}}. \quad (6)$$

$$\nu_{y_k^s,t} = \frac{P_s h_{y_k} \|x_k^s\|^{-\alpha}}{\varrho + \sum_{x_i^s \in \Phi_s \setminus x_k^s} P_s \rho_{s,t} h_{y_i} \|x_i^s\|^{-\alpha} + \sum_{x_i^p \in \Phi_p} P_p \rho_{p,t} h_{x_i} \|x_i^p\|^{-\alpha}}. \quad (7)$$

$$\mu_{y_k^p} = e^{-\frac{\theta_p x^\alpha}{\varphi}} - \frac{2\pi^2}{\alpha \sin(\frac{2\pi}{\alpha})}\left[\lambda_p^1(\theta_p x^\alpha)^{\frac{2}{\alpha}} + \lambda_s^1(\theta_p \vartheta x^\alpha)^{\frac{2}{\alpha}}\right], \tag{11}$$

where $\lambda_p^1 = \lambda_p p_1$ with $p_1 = x_i^p$ defined as the non-empty probability of any primary priority queue (located outside $L \in R^2$). Similarly, $\lambda_s^1 = \lambda_s p_2$, where $p_2 = x_0^p x_i^s$ provides the active probability of the secondary queue (located outside $L \in R^2$), which is defined as the joint probability of an empty primary priority queue and non-empty secondary priority queue.

*Proof:* The proof is straightforward from Lemma 1 and is presented in Appendix B.

Similar to the case of the primary network, the conditional coverage probability at any typical SR in any time slot $t$ is given as

$$\mu_{y_k^s,t} = P(\nu_{y_k^s,t} \geq \theta_s | \Phi, \forall \Phi = \Phi_p \cup \Phi_s). \tag{12}$$

*Lemma 3:* Given that a tagged SR is located at $y_k^s \in \Phi_s$ and conditioned on the spatial realization $\Phi = \Phi_p \cup \Phi_s$, the coverage probability in any time slot $t$ is expressed as

$$\mu_{y_k^s,t} = e^{-\frac{\theta_s \|x_k^s\|^\alpha \varrho}{P_s}} \prod_{x_i^s \in \Phi_s \setminus x_k^s} \left(1 - \frac{E[\rho_{s,t}|\Phi]}{1 + \|x_i^s\|^\alpha / \theta_s \|x_k^s\|^\alpha}\right) \times \prod_{x_i^p \in \Phi_p} \left(1 - \frac{(1/\vartheta)E[\rho_{p,t}|\Phi]}{1 + \|x_i^p\|^\alpha / \theta_s \|x_k^s\|^\alpha}\right). \tag{13}$$

Considering a special case where all classes of transmitters transmit with the same transmit power, the conditional coverage probability as $\varrho \to 0$ is reduced to

$$\mu_{y_k^s,t} = \prod_{x_i^s \in \Phi_s \setminus x_k^s} \left(1 - \frac{E[\rho_{s,t}|\Phi]}{1 + \|x_i^s\|^\alpha / \theta_s \|x_k^s\|^\alpha}\right) \times \prod_{x_i^p \in \Phi_p} \left(1 - \frac{E[\rho_{p,t}|\Phi]}{1 + \|x_i^p\|^\alpha / \theta_s \|x_k^s\|^\alpha}\right). \tag{14}$$

*Proof:* The proof is similar to the proof of Lemma 1 and is omitted for brevity.

In order to derive the closed-form expression for $\mu_{y_k^s,t}$, we follow Assumption 1 as in the PU's case. In this case, a typical ST may be located in the secondary queue or virtual queue if it has previously been interrupted by primary activities.

*Lemma 4:* The coverage probability of a tagged ST in a secondary or virtual queue located within region $L \in R^2$ is given as

$$\mu_{y_k^s} = e^{-\frac{\theta_s x^\alpha \varrho}{P_s}} - \frac{2(\pi x)^2}{\alpha \sin(\frac{2\pi}{\alpha})}\left[\lambda_s^1 \theta_s^{\frac{2}{\alpha}} + \lambda_p^1 (\frac{\theta_p}{\vartheta})^{\frac{2}{\alpha}}\right]. \tag{15}$$

*Proof:* The expression is obtained by applying the probability generating functional (PGFL) of PPP in the polar coordinate form to Lemma 3. The proof is similar to Appendix B and is omitted for brevity.

### B. VACATION-BASED PRE-EMPTIVE PRIORITY QUEUEING SYSTEM

We now describe the details of the queueing system adopted in this work. As mentioned in Section II, a typical *uth* priority queue is said to be on vacation whenever the channel is unavailable for its usage - on vacation, i.e. when the channel is serving a higher priority queue. Although we considered three priority queues - primary, virtual and secondary queues, where interrupted ST enjoys priority over the newly arrived STs and is immediately placed in the virtual queue after interruption, a careful observation of the system shows that there can only be one ST in the virtual queue at any time, which makes it very easy to analyze. As a result of this, the virtual queue can be seen as part of the secondary queue in which any interrupted ST is simply returned to the head of the secondary queue and resumes its interrupted transmission in the next slot when the primary queue is empty. Hence, there are only two possible arrivals into the system - $\xi_p$ and $\xi_s$. We henceforth focus on primary and secondary queues.

*Assumption 2:* The inter-class arrivals at any time slot are assumed to be independent and identically distributed.

*Remarks:* The analysis in both primary and secondary classes can be dependent. However, in our case, we considered a typical CRN in which PUs and SUs arrivals are independent. We further assumed that there is no correlation between the number of primary and secondary transmitters arriving during the same slot, so as to allow us to investigate the performance of each *uth* priority queue separately.

It is easy to observe that the primary priority queue is not affected by the secondary priority queue because of the pre-emptive priority access possessed by the primary queue. Hence, the primary queue can be modeled as Geo/Geo/1 where PUs' service time is considered to follow the geometric distribution. In such a case, the transmission matrix representing the primary queue can be given as

$$P_1 = \begin{pmatrix} \bar{\xi_p} & \xi_p & & \\ \bar{\xi_p}\mu_{y_k^p} & \bar{\xi_p}\bar{\mu_{y_k^p}} + \xi_p \mu_{y_k^p} & \xi_p \bar{\mu_{y_k^p}} & \\ & \bar{\xi_p}\mu_{y_k^p} & \bar{\xi_p}\bar{\mu_{y_k^p}} + \xi_p \mu_{y_k^p} & \xi_p \bar{\mu_{y_k^p}} \\ & & \ddots & \ddots \end{pmatrix}, \tag{16}$$

where the probability of having $i$ PTs $x_i$ obtained from the steady-state distribution $x = [x_0, x_1, x_2, \ldots]$ is given as $x_i = R^i \frac{x_0}{\bar{\mu_{y_k^p}}}$ with $R = \frac{\xi_p \bar{\mu_{y_k^p}}}{\bar{\xi_p}\mu_{y_k^p}}$ and $x_0 = \frac{\mu_{y_k^p} - \xi_p}{\mu_{y_k^p}}$ [12]. From this, the mean time in the queue [23] can be obtained as

$$E[W_q] = \frac{\xi_p \bar{\xi_p}}{\mu_{y_k^p}(\mu_{y_k^p} - \xi_p)}, \tag{17}$$

while the average waiting time in the system is given as $E[W] = E[W_q] + \frac{1}{\mu_{y_k^p}}$.

However, owing to the limitation of geometric service time - lack of memory [23], modeling of the system considered

using geometry service time is inappropriate, since the secondary queue's performance is affected by the arrival rate and service time at the primary queue. Hence, the performance at the primary queue needs to be incorporated into the modeling of the secondary queue. We therefore characterize both primary and secondary queues using the 2D Geo/G/1 DTMC model and characterize any typical user's service time as a non-negative random variable. A user can then be said to have a general service time S with mean $E[S] = \frac{1}{\mu}$, while the second moment of each user's service time is given as $E[S^2]$.

If the existence of a steady-state is assumed, then $x = [x_0, x_1, x_2, \ldots]$ is given as

$$x = xP, x1 = 1. \tag{18}$$

Similarly, the stationary distribution equations of the embedded Markov chain can be captured as

$$x_i = x_0\xi_i + \sum_{j=1}^{i+1} x_j\xi_{i-j+1}, \quad i \geq 0, \tag{19}$$

where $\xi_i$ can be defined as the probability that the number of arrivals on the *uth* priority queue during the service time of the *nth* transmitter belonging to the *uth* priority class is *i* and *P* is given as [23]

$$P = \begin{pmatrix} \xi_0 & \xi_1 & \xi_2 & \cdots \\ \xi_0 & \xi_1 & \xi_2 & \cdots \\ & \xi_0 & \xi_1 & \cdots \\ & & \xi_0 & \cdots \\ & & \vdots & \cdots \end{pmatrix}. \tag{20}$$

At the primary priority queue, $x_0 = 1 - \frac{\xi_p}{\mu_k^p}$, while at the secondary queue, $x_0 = 1 - \frac{\xi_s}{\mu_k^s}$. The inter-dependence between $x_0$ and $\mu_k$ results in causality problems [12] and can only be solved using an iterative solution or by simply obtaining necessary and sufficient conditions for stability. According to (17), the mean time a tagged transmitter spends in the system can generally be represented as

$$W = \frac{1}{\mu_k} + \frac{\xi E[S^2]}{2(1 - \xi E[S])}. \tag{21}$$

This is fundamental to the analysis in the next section.

## IV. PERFORMANCE ANALYSIS

In this section, we analyzed the delay experienced by primary and secondary users. A typical SU experience includes the time in which its transmission was interrupted by PUs. We considered primary and secondary queues of infinite capacities and assumed that the system is stable, i.e. the overall traffic intensity $\tau = \tau_p + \tau_s < 1$, where $\tau_p = \frac{\xi_p}{\mu_{y_k^p}}$ and $\tau_s = \frac{\xi_s}{\mu_{y_k^s}}$ are the intensities at the primary and secondary priority queues respectively. The analysis in this section will be used to investigate users' QoS in the network.

### A. DELAY ANALYSIS IN THE PRIMARY NETWORK

The delay experienced by any tagged PT is the mean time such a PT spends in the system (which is equivalent to the service time and time spent in the queue). As in the case of Geo/Geo/1, the waiting time in the primary queue is straightforward, since arrival and service in the secondary queue do not affect PUs' channel usage. The primary queue can be modeled as a queueing system without priority. It is, however, possible that a tagged PT does not immediately start transmission upon arrival at the system, depending on the primary queue traffic intensity, and may have to wait in the primary queue until all PTs with early arrival times leave the system, following the FCFS approach. Hence, the mean delay experienced by any tagged PT depends not only on its arrival and service times, but also on the overall traffic intensity at the primary queue. From the equivalent discrete time Geo/G/1 queueing system without priority obtained in [10], [25]–[27], it is clear that the mean delay experienced by a tagged PT can be obtained, as presented in Proposition 1.

*Proposition 1:* The mean delay experienced by any typical PT $x_k^p \in \Phi_p$ expressed as the average number of slots between the end of its arrival and departure slots is given as

$$D_p^{\Phi} = \frac{\tau_p - \frac{\xi_p^2}{\mu_{y_k^p}}}{\tau_p(\mu_{y_k^p} - \xi_p)}. \tag{22}$$

*Proof:* The derivation is straightforward from the general structure of the Geo/G/1 queueing model given in (21).

### B. DELAY ANALYSIS IN THE SECONDARY NETWORK

The delay experienced by any tagged ST includes the mean time spent in the secondary queue, the actual service time and the time spent in the virtual queue owing to service interruption (because of the pre-emptive priority discipline adopted, an interrupted ST resumes its transmission during the next slot if the primary queue is empty). The actual time spent in the virtual queue is complicated because of its dependence on the primary queue. With Assumption 2, it is clear that we can analyze the performance of primary and secondary queues separately. In order to obtain analysis for the queueing system with possible interrupted services, it is important to obtain a stochastic analysis of the perceived interruption process for any typical ST. We hence adopted queueing models with service interruptions [27]–[29] to account for the overall time spent in the virtual queue because of PTs' activities.

Let *a* be defined as the probability that the channel remains in the state of absorption, hence available for the secondary priority queue during the next slot, provided that it was available at the beginning of the present slot. Careful observation of the system shows that the interruption experienced by a tagged ST can be modeled as a Bernoulli process. Hence the lengths of the periods during which the channel is available

for secondary priority users follows a geometric distribution with mean $\frac{1}{1-a}$, while the mean length of the slots in which the secondary queue perceives the channel as being on vacation is given as

$$v = \frac{\tau_p}{(1-\tau_p)(1-a)}. \tag{23}$$

The effective service time of any tagged ST is hence given as $\mu_e = \frac{1}{\mu_{y_k^s}\psi}$, $\psi$ being the fraction of time in which the channel is available for secondary transmissions, given as $\psi = \frac{1}{1+v-av}$. The analysis of the mean delay experienced by any tagged ST is presented in Proposition 2.

*Proposition 2:* The mean delay experienced by any typical ST $x_k^s \in \Phi_s$ is given as

$$D_s^{\Phi} = \frac{(1-a)}{2}\left\{\psi\beta_v + \frac{\mu_e}{1-a} - v(1-a\psi v) + \frac{\mu_e\beta_{\xi_s}+\xi_s^2\beta_{\mu_e}}{2\xi_s(1-\tau)}\right\}, \tag{24}$$

where $\beta_{[.]}$ is the variance of [.].

*Proof:* The proof is straightforward from [27]–[29] and is summarized in Appendix C for completeness.

### C. QoS ANALYSIS

We defined QoS as the probability that the delay tolerance limit of a typical transmitter under consideration is satisfied, i.e.

$$QoS = P(D_{u,0}^{\Phi} \le \chi). \tag{25}$$

Let the maximum expected delay of a typical transmitter be denoted as $\chi$, then the QoS of such transmitter is satisfied if the delay experienced is not more than $\chi$, otherwise its QoS requirement is not satisfied. It can also be interpreted as the fraction of transmitters belonging to any typical priority class that required at most $\chi$ time slot(s) to complete their services. When the QoS requirement is not satisfied, a typical transmitter is said to have taken more time slot than desirable to complete its transmission, which can have negative influence on its satisfaction and service.

#### 1) PRIMARY PRIORITY QUEUE

The QoS of any tagged PT can be expressed as

$$\begin{aligned} QoS_p &= P(D_{p,0}^{\Phi} \le \chi), \\ &= 1 - F_0^{\Phi}\Big(\frac{1-\xi_p}{\chi} + \xi_p\Big), \end{aligned} \tag{26}$$

where $F_0^{\Phi}(u) = \frac{1}{2} - \frac{1}{\pi}\int_0^{\infty}\frac{1}{w}\mathcal{Q}\{u^{-jw}M_{Y_0^{\Phi}}(jw)\}dw$. $\mathcal{Q}\{z\}$ is the imaginary part of the complex number $z$ and $M_{Y_0^{\Phi}}$ is given as

$$\begin{aligned} M_{Y_0^{\Phi}}(s)\exp\Big(&-(\lambda_p+\lambda_s)\theta_p^{\delta}r_p^2\frac{\pi^2\delta}{\sin(\pi\delta)} \\ &\times\sum_{k=1}^{\infty}\binom{s}{k}\frac{\Gamma(\delta)}{\Gamma(k)\Gamma(\delta-k+1)}p^k\Big). \end{aligned} \tag{27}$$

$F_0^{\Phi}(u)$ is the Gil-Pelaez theorem [30] and its derivation can be found in [2], [31]–[33]. The proof of (27) is summarized in Appendix D for completeness.

#### 2) SECONDARY PRIORITY QUEUE

Similarly, the QoS of any tagged ST can be expressed as

$$QoS_s = P(D_{s,0}^{\Phi} \le \chi). \tag{28}$$

Expressing Proposition 2 as a subject of $\mu_{y_k^s}$ is difficult. Hence, we obtained only an approximate representation of $Qos_s$ given as;

$$\begin{aligned} QoS_s \approx 1 - F_0^{\Phi} \\ \times\left(\frac{\frac{5\beta_{\xi_s}}{4\xi_s}+0.5}{\psi\Big[\mu_e - \frac{(1-a)}{2}\psi\beta_v + \frac{v}{2}(1-a)(1-a\psi v) - \frac{2\xi_s}{5}\Big]}\right). \end{aligned} \tag{29}$$

## V. NUMERICAL RESULTS AND SIMULATION

We now present the results of the analysis presented in the previous sections. Except when stated otherwise, the following parameters were used in the simulations: $\lambda_s = 0.3$, $\lambda_p = 0.03$, $r_p = ||y_k^p|| = 0.5$, $r_s = ||y_k^s|| = 0.1$, $P_p = 0\ dB$, $P_s = -32\ dB$, $\alpha = 4$, and $W = -180\ dB$.

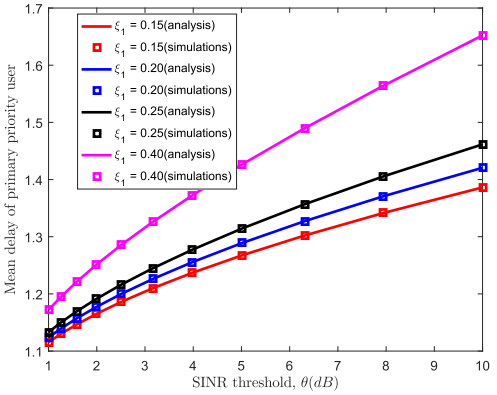


**FIGURE 2.** Mean delay experienced in primary priority queue.

Fig. 2 and Fig. 3 show the effects of the SINR threshold requirement on the mean delay experienced by users in the network. As the SINR threshold increases, coverage is expected to reduce, provided that interference and noise on the network remain unchanged. This confirms that a decrease in coverage probability further reduces the transmission success of users, hence increasing the probability of retransmission. Although the arrival rate of PTs (delay-sensitive users) is not expected to be higher than that of STs (which are delay-tolerance users), the average delay experienced by any typical ST increases with the arrival rate of any user's priority class, while the average delay experienced by any typical PT increases with the arrival rate at the primary priority queue. With a higher arrival rate, users spend more time in the queue, hence increasing the mean delay experience.

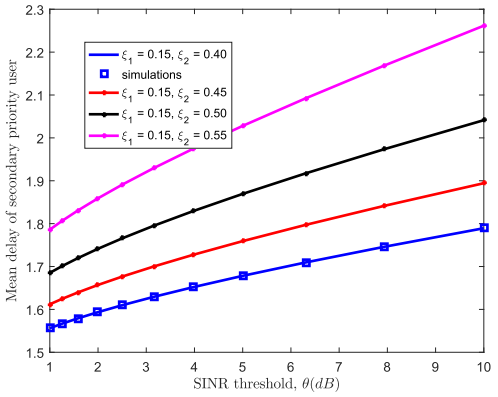


**FIGURE 3.** Mean delay experienced in secondary priority queue.

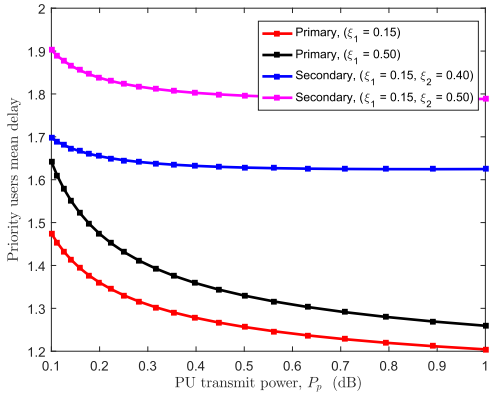


**FIGURE 4.** Effect of transmit power on the network mean delay, $\theta = 9.5$ *dB*.

As expected, an increase in PTs' transmit power reduces the overall mean delay in the network, confirming the reliability of our approach, as shown in Fig. 4. With an increase in PTs' transmit power, coverage is expected to be increased in the primary network, hence improving the service completion rate in the primary network. Because of the pre-emptive priority access of the PTs, a poor service completion rate at the primary network means that STs will spend more time in the secondary queue, while interrupted STs are also expected to spend increased time in the virtual queue (or simply at the head of the secondary queue). The mean time spent by STs is also expected to decrease with an increase in STs transmit power.

We defined QoS as the probability that the total time spent by any typical user in the network would be below a predefined threshold. As shown in Fig. 5, the more delay-tolerant any network is, the better its QoS. At a constant QoS threshold requirement, the user's QoS experience reduces with more service time. Interestingly, users' QoS experience improves with lower network arrival rates, as shown in Fig. 6, which confirms the effects of delay on users' experiences in both priority classes. Similarly, a lower arrival rate at the primary queue further improves users' experiences in the secondary network, since less time will be spent in the secondary queue waiting for transmission opportunities and the virtual queue in case of interruption.

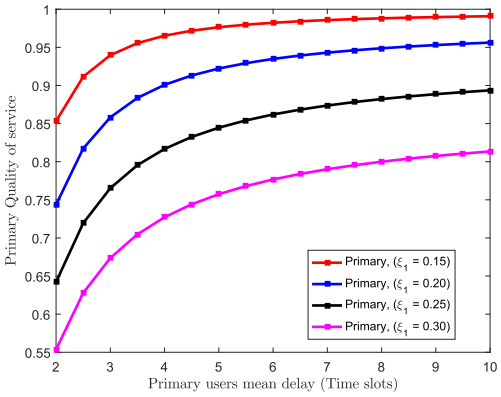


**FIGURE 5.** QoS at the primary priority queue, $\theta = 9.5$ *dB*.

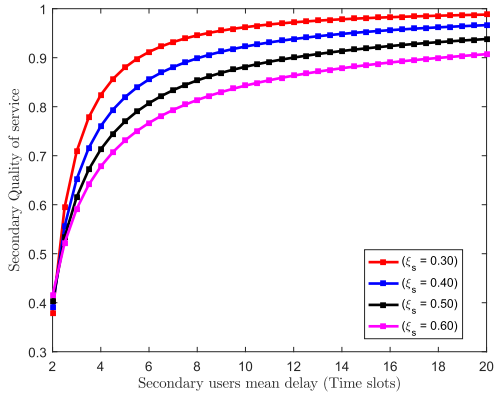


**FIGURE 6.** QoS at the secondary priority queue, $\theta = 9.5$ *dB*, $\xi_p = 0.10$.

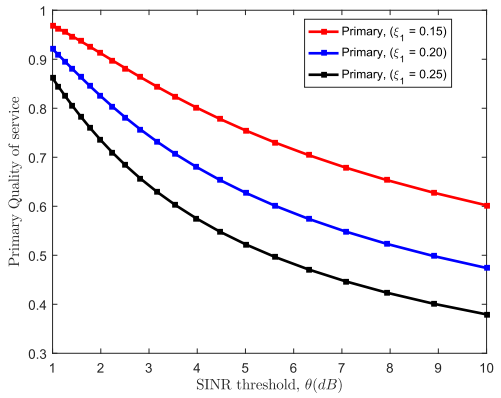


**FIGURE 7.** Effects of $\theta$ on users' experience, $\chi = 2$.

We also investigate the effect of the SINR threshold on users' experiences, as presented in Fig. 7. An increase in the SINR threshold is expected to decrease the service completion rate, which will further degrade users' experience. Generally, a lower arrival rate at the primary queue implies that the probability of causing interruption at the secondary queue reduces, which further reduces STs' delay experiences.

## VI. CONCLUSION

This paper presents a spatiotemporal characterization of users' experience in a massive CRN. To capture the intrinsic characteristic of CRN, the primary priority queue was

considered to have pre-emptive priority over both the virtual and secondary priority queues. The virtual queue was further considered to have priority over the secondary priority queue. Careful observation of the network, however, shows that the virtual queue should rather be regarded as part of the secondary queue, to avoid unnecessarily complicated analysis. The performance of the network was carried out using delay experienced by a typical user in each priority class, while expressions for users' QoS were derived.

Stochastic geometry and queueing theory were combined to obtain spatiotemporal analysis of users' experience. The analysis shows the interdependence between the components of the SG and queueing theory. The work presented in this paper is useful, especially as more users will be connected in the near future owing to the continuous evolution in wireless communications. Through this, cognitive users/devices can be allowed to access the scarce spectrum resources based on their class priority. The analyses presented in this work are useful in managing and understanding users' experience, which are important for the next generation of users. In the future, it may be interesting to model the corresponding arrival processes using the late arrival system in order to observe the effects of such system on the network performance.

## APPENDIXES

## APPENDIX A
## PROOF OF LEMMA 1

From (8), we know that (30), as shown at the bottom of this page.

With Rayleigh fading assumption,

$$\mu_{y_k^p,t} = e^{-\frac{\theta_p \|x_k^p\|^\alpha}{\varphi}} \left( E\left\{ \prod_{x_i^p \in \Phi_p \setminus x_k^p} \exp\left( -\theta_p \|x_k^p\|^\alpha \frac{\rho_{p,t} h_{x_i}}{\|x_i^p\|^\alpha} \right) \right\} \times E\left\{ \prod_{x_i^s \in \Phi_s} \exp\left( -\theta_p \|x_k^p\|^\alpha \frac{\vartheta \rho_{s,t} h_{y_i}}{\|x_i^s\|^\alpha} \right) \right\} | \Phi \right). \quad (31)$$

With some algebraic manipulations, Lemma 1 is obtained. This completes the proof.

## APPENDIX B
## PROOF OF LEMMA 2

Since we considered a massive CRN, two types of interference are possible - intra-network and inter-network interference. A typical PR receiving service from the tagged PT will hence experience interference from neighbouring PTs and STs. After Assumption 1 had been applied to Lemma 1, we further applied the PGFL of PPP in the polar coordinate form. The Laplace transform (LT) of interference received at the typical PR from neighbouring PTs is then obtained as

$$\mathcal{L}_{I_{pp}}(s) = \exp\left\{ -2\pi\lambda_p^1 \int_0^\infty \frac{x}{1 + \frac{x^\alpha}{sP_p}} dx \right\}, \quad (32)$$

while the LT of interference received from the neighbouring STs is obtained as

$$\mathcal{L}_{I_{sp}}(s) = \exp\left\{ -2\pi\lambda_s^1 \int_0^\infty \frac{x}{1 + \frac{x^\alpha}{sP_s}} dx \right\}. \quad (33)$$

At $s = \frac{\theta_p}{P_p x^{-\alpha}}$, the proof of lemma 2 is obtained.

## APPENDIX C
## PROOF OF PROPOSITION 2

Recall that a typical ST is assumed to have a random number of packets to transmit and each of those packets requires one slot to be transmitted, provided that the transmission is successful, without retransmission. The effective service time of the tagged ST is hence the time period between the beginning of the slot during which the first packet is transmitted and the end of the slot during which the last packet of the same tagged ST is successfully transmitted. It is clear from such a definition that the effective service time includes the time spent in the virtual queue (due to possible interruptions from the primary priority queue).

We define the unfinished service in the secondary queue at the beginning of any slot $t$ as the number of slots required to serve all STs in the system, assuming no new arrival at the secondary queue. The analysis for such a parameter can be obtained from (3) as

$$W_s(t+1) = [W_s(t) - D_s(t)]^+ + \sum_{k=1}^{n_s^{(t)}} \mu_k, \quad (34)$$

where $n_s^{(t)}$ is the number of STs that arrived during the slot $t$ and $\mu_k$ is the effective service time of the *kth* ST, which arrived in slot $t$. According to [27], the probability generating function (pgf) of $W_s$ while assuming an equilibrium system, is given as

$$W_s(z) = \frac{\psi}{\varpi}(1-\tau_f)\frac{zH(z) - n_s(\mu_e(z))}{z - n_s(\mu_e(z))}, \quad (35)$$

$$\begin{aligned}
\mu_{y_k^p,t} &= P(\nu_{y_k^p,t} \geq \theta_p | \Phi, \forall \Phi = \Phi_p \cup \Phi_s), \\
\mu_{y_k^p,t} &= P\left( \frac{P_p h_{x_k} \|x_k^p\|^{-\alpha}}{\varrho + \sum_{x_i^p \in \Phi_p \setminus x_k^p} P_p \rho_{p,t} h_{x_i} \|x_i^p\|^{-\alpha} + \sum_{x_i^s \in \Phi_s} P_s \rho_{s,t} h_{y_i} \|x_i^s\|^{-\alpha}} \geq \theta_p | \Phi \right), \\
&= P\left( h_{x_k} \geq \frac{\theta_p \|x_k^p\|^\alpha}{P_p} \left[ \varrho + \sum_{x_i^p \in \Phi_p \setminus x_k^p} P_p \rho_{p,t} h_{x_i} \|x_i^p\|^{-\alpha} + \sum_{x_i^s \in \Phi_s} P_s \rho_{s,t} h_{y_i} \|x_i^s\|^{-\alpha} \right] | \Phi \right). \quad (30)
\end{aligned}$$

where $\varpi$ is the probability that the channel is available at the preceding slot and $\tau_f = \tau < 1$ is the effective traffic intensity for pre-emptive resume discipline. The definition of $H(z)$ is provided in [27]. By taking $n_s$ as the number of STs that arrived in the same slot but before the tagged ST, it is clear that the delay experienced by a tagged ST can be obtained from (34) as

$$D_s(t+1) = [W_s(t) - 1]^+ + \sum_{k=1}^{n_s+1} \mu_k. \tag{36}$$

By obtaining the pgf of $\xi_s$ and then $D_s$, Proposition 2 is obtained.

## APPENDIX D
## PROOF OF (27)

For a typical PT $x_k^p \in \Phi_p$ located at the center of a disk, the success probability conditioned on $\Phi = \Phi_p \cup \Phi_s$ is given as

$$\begin{aligned} P^{x0}(\mu_k^p) &= pP^{x0}(\nu_{y_k^p,t} > \theta_p|\Phi) \\ &= pE^{x0}\Bigg\{ \exp\Bigg( -\frac{\theta_p r_p^\alpha \varrho}{P_p} - \sum_{x_i^p \in \Phi_p \setminus x_k^p} h_{x_k} \theta_p r_p^\alpha \|x_k^p\|^{-\alpha} \\ &\quad - \sum_{x_i^s \in \Phi_s} \frac{P_s}{P_p} h_{x_k} \theta_p r_p^\alpha \|x_i^s\|^{-\alpha} \Bigg) | \Phi \Bigg\}, \end{aligned} \tag{37}$$

with $P_p = P_s$ and $\varrho \to 0$ as in the simplified CRN and by applying Rayleigh fading assumption,

$$\begin{aligned} P^{x0}(\mu_k^p) = &\prod_{x_i^p \in \Phi_p \setminus x_k^p} \left( \frac{p}{1 + \theta_p r_p^\alpha \|x_k^p\|^{-\alpha}} + 1 - p \right) \\ &\times \prod_{x_i^s \in \Phi_s} \left( \frac{p}{1 + \theta_p r_p^\alpha \|x_i^s\|^{-\alpha}} + 1 - p \right). \end{aligned} \tag{38}$$

From the moment generating function of $Y_0^\Phi \triangleq \ln(P^{x0}(\mu_k^p))$, we know that

$$M_{Y_0^\Phi}(s) = E[\exp(s \ln(P^{x0}(\mu_k^p)))].$$

By applying the PGFL of PPP,

$$\begin{aligned} M_{Y_0^\Phi}(s) = \exp\Bigg[ &- \lambda_p \int_{R^2} \left( 1 - \left( \frac{p}{1 + \theta_p r_p^\alpha \|x_k^p\|^{-\alpha}} - p \right)^s \right) dx \\ &- \lambda_s \int_{R^2} \left( 1 - \left( \frac{p}{1 + \theta_p r_p^\alpha \|x_i^s\|^{-\alpha}} + 1 - p \right)^s \right) dx \Bigg]. \end{aligned} \tag{39}$$

We can express the moment as $M_{Y_0^\Phi}(s) = \exp(-(\lambda_p + \lambda_s) F_0)$. By making $\delta = \frac{2}{\alpha}$ and with some algebraic manipulation, $M_{Y_0^\Phi}(s)$ is obtained.

## REFERENCES

[1] H. H. Yang and T. Q. S. Quek, "Spatio-temporal analysis for SINR coverage in small cell networks," *IEEE Trans. Commun.*, vol. 67, no. 8, pp. 5520–5531, Aug. 2019.
[2] Y. Zhong, M. Haenggi, T. Q. S. Quek, and W. Zhang, "On the stability of static Poisson networks under random access," *IEEE Trans. Commun.*, vol. 64, no. 7, pp. 2985–2998, Jul. 2016.
[3] X. Song, C. Yin, D. Liu, and R. Zhang, "Spatial throughput characterization in cognitive radio networks with threshold-based opportunistic spectrum access," *IEEE J. Sel. Areas Commun.*, vol. 32, no. 11, pp. 2190–2204, Nov. 2014.
[4] X. Song, C. Yin, D. Liu, and R. Zhang, "Spatial opportunity in cognitive radio networks with threshold-based opportunistic spectrum access," in *Proc. IEEE Int. Conf. Commun. (ICC)*, Budapest, Hungary, Jun. 2013, pp. 2695–2700.
[5] U. Tefek and T. J. Lim, "Interference management through exclusion zones in two-tier cognitive networks," *IEEE Trans. Wireless Commun.*, vol. 15, no. 3, pp. 2292–2302, Mar. 2016.
[6] A. Busson, B. Jabbari, A. Babaei, and V. Veque, "Interference and throughput in spectrum sensing cognitive radio networks using point processes," *J. Commun. Netw.*, vol. 16, no. 1, pp. 67–80, Feb. 2014.
[7] C. Rattaro, P. Bermolen, F. Larroca, and P. Belzarena, "A stochastic geometry analysis of multichannel cognitive radio networks," in *Proc. 9th Latin Amer. Netw. Conf. (LANC)*, Valparaiso, In, USA, Oct. 2016, pp. 32–38.
[8] T. V. Nguyen and F. Baccelli, "A probabilistic model of carrier sensing based cognitive radio," in *Proc. IEEE Symp. New Frontiers Dyn. Spectr. (DySPAN)*, Singapore, Apr. 2010, pp. 1–12.
[9] H. H. Yang, G. Geraci, Y. Zhong, and T. Q. S. Quek, "Packet throughput analysis of static and dynamic TDD in small cell networks," *IEEE Wireless Commun. Lett.*, vol. 6, no. 6, pp. 742–745, Dec. 2017.
[10] H. H. Yang, Y. Wang, and T. Q. S. Quek, "Delay analysis of random scheduling and round robin in small cell networks," *IEEE Wireless Commun. Lett.*, vol. 7, no. 6, pp. 978–981, Dec. 2018.
[11] Y. Zhong, T. Q. S. Quek, and X. Ge, "Heterogeneous cellular networks with spatio-temporal traffic: Delay analysis and scheduling," *IEEE J. Sel. Areas Commun.*, vol. 35, no. 6, pp. 1373–1386, Jun. 2017.
[12] M. Gharbieh, H. ElSawy, A. Bader, and M.-S. Alouini, "Spatiotemporal stochastic modeling of IoT enabled cellular networks: Scalability and stability analysis," *IEEE Trans. Commun.*, vol. 65, no. 8, pp. 3585–3600, May 2017.
[13] N. Jiang, Y. Deng, X. Kang, and A. Nallanathan, "Random access analysis for massive IoT networks under a new spatio-temporal model: A stochastic geometry approach," *IEEE Trans. Commun.*, vol. 66, no. 11, pp. 5788–5803, Nov. 2018.
[14] K. Stamatiou and M. Haenggi, "Random-access Poisson networks: Stability and delay," *IEEE Commun. Lett.*, vol. 14, no. 11, pp. 1035–1037, Nov. 2010.
[15] Y. Gu, C. Li, B. Xia, D. Xu, and Z. Chen, "Modeling and performance analysis of stochastic mobile edge computing wireless networks," in *Proc. IEEE 89th Veh. Technol. Conf. (VTC-Spring)*, Kuala Lumpur, Apr. 2019, pp. 1–5.
[16] S. Wang, J. Zhang, and L. Tong, "Delay analysis for cognitive radio networks with random access: A fluid queue view," in *Proc. IEEE INFOCOM*, Mar. 2010, pp. 1–9.
[17] J. Xin, Q. Zhu, G. Liang, and T. Zhang, "Performance analysis of D2D underlying cellular networks based on dynamic priority queuing model," *IEEE Access*, vol. 7, pp. 27479–27489, 2019.
[18] L. Chen, L. Huang, H. Xu, and Y. Du, "Queueing analysis for preemptive transmission in underlay CRNs," *Int. J. Commun. Syst.*, vol. 29, no. 6, pp. 1138–1155, Apr. 2016.
[19] S. Hoque, S. Shekhar, D. Sen, and W. Arif, "Analysis of handoff delay for proactive spectrum handoff scheme with PRP M/G/1/K queuing system in cognitive radio networks," *IET Commun.*, vol. 13, no. 6, pp. 706–711, Apr. 2019.
[20] W. Jiao, G. Liu, K.-S. Lui, and M. Sheng, "Queue performance of cognitive radio networks with general primary user activity model," *IET Commun.*, vol. 9, no. 15, pp. 1821–1828, Oct. 2015.
[21] A. G. M. Ali, E.-S. Ahmed Youssef, M. R. M. Rizk, M. Salman, and K. G. Seddik, "Cooperative delay-constrained cognitive radio networks: Delay-throughput trade-off with relaying full-duplex capability," *IEEE Access*, vol. 8, pp. 9157–9171, 2020.
[22] M. Emara, H. ElSawy, and G. Bauch, "Prioritized multi-stream traffic in uplink IoT networks: Spatially interacting vacation queues," 2019, *arXiv:1907.07888*. [Online]. Available: http://arxiv.org/abs/1907.07888

[23] A. S. Alfa, *Applied Discrete-Time Queues*. New York, NY, USA: Springer, 2016.
[24] A. S. Alfa, "Discrete time queues and matrix-analytic methods," *Top*, vol. 10, no. 2, pp. 147–185, Dec. 2002.
[25] G. Wang, Y. Zhong, R. Li, X. Ge, T. Q. S. Quek, and G. Mao, "Effect of spatial and temporal traffic statistics on the performance of wireless networks," 2018, *arXiv:1804.06754*. [Online]. Available: http://arxiv.org/abs/1804.06754
[26] I. Atencia and P. Moreno, "A discrete-time Geo/G/1 retrial queue with general retrial times," *Queueing Syst.*, vol. 48, nos. 1–2, pp. 5–21, Sep. 2004.
[27] J. Walraevens, D. Fiems, and H. Bruneel, "Performance analysis of priority queueing systems in discrete time," in *Network Performance Engineering*. Berlin, Germany: Springer, 2011, pp. 203–232.
[28] Heines, "Buffer behavior in computer communication systems," *IEEE Trans. Comput.*, vols. C-28, no. 8, pp. 573–576, Aug. 1979.
[29] D. Fiems, B. Steyaert, and H. Bruneel, "Performance evaluation of CAI and RAI transmission modes in a GI-G-1 queue," *Comput. Oper. Res.*, vol. 28, no. 13, pp. 1299–1313, Nov. 2001.
[30] J. Gil-Pelaez, "Note on the inversion theorem," *Biometrika*, vol. 38, nos. 3–4, pp. 481–482, Dec. 1951.
[31] H. H. Yang and T. Q. S. Quek, "SIR coverage analysis in cellular networks with temporal traffic: A stochastic geometry approach," 2018, *arXiv:1801.09888*. [Online]. Available: http://arxiv.org/abs/1801.09888
[32] M. Haenggi and R. Smarandache, "Diversity polynomials for the analysis of temporal correlations in wireless networks," *IEEE Trans. Wireless Commun.*, vol. 12, no. 11, pp. 5940–5951, Nov. 2013.
[33] M. Haenggi, "The meta distribution of the SIR in Poisson bipolar and cellular networks," *IEEE Trans. Wireless Commun.*, vol. 15, no. 4, pp. 2577–2589, Apr. 2016.

**SAMUEL D. OKEGBILE** (Student Member, IEEE) received the B.Tech. degree (Hons.) in computer engineering from the Ladoke Akintola University of Technology, Ogbomoso, Nigeria, in 2011, and the M.Sc. degree (Hons.) in computer science from Obafemi Awolowo University, Ile-Ife, Nigeria, in 2016. He is currently pursuing the Ph.D. degree in computer engineering with the Department of Electrical, Electronic, and Computer Engineering, University of Pretoria, South Africa. His research interests include pervasive and mobile computing which includes various interesting topics on cognitive radio networks, the Internet of Things, and wireless sensor networks.

**BODHASWAR T. MAHARAJ** (Senior Member, IEEE) received the Ph.D. degree in wireless communications from the University of Pretoria, South Africa. He is currently a Professor and holds the position of Sentech Chair of broadband wireless multimedia communications with the Department of Electrical, Electronic, and Computer Engineering, University of Pretoria. His research interests include MIMO channel modeling, OFDM-MIMO systems, and cognitive radio for rural broadband.

**ATTAHIRU S. ALFA** (Member, IEEE) is currently a Professor Emeritus with the Department of Electrical and Computer Engineering, University of Manitoba, and also an Extraordinary Professor with the Department of Electrical, Electronic, and Computer Engineering, University of Pretoria. He has carried out applied research for Nortel Networks, Bell-Northern Research, TRLabs (now TRTech), Bell Canada, Winnipeg Regional Health Authority, Motorcoach Industries, and several other industries. He has authored the books, *Queueing Theory for Telecommunications: Discrete Time Modelling of a Single Node System* (Springer, 2010) and *Applied Discrete Time Queueing Theory* (Springer, 2015). His researches include, but not limited to, the following areas: performance analysis and resource allocation in telecommunication systems, modeling of communication networks, queueing theory, optimization, the analysis of cognitive radio networks, modeling and analysis of wireless sensor networks, developing efficient decoding algorithms for LDPC codes, channel modeling, traffic estimation for the Internet, and cross layer analysis. He also involved in the application of queueing theory to other areas, such as transportation systems, manufacturing systems, and healthcare systems. He was the NSERC Chair of tele-traffic, from 2004 to 2012.